MOBILIZATION OF A DEPOSITED PARTICLE BY A MOVING LIQUID-LIQUID INTERFACE AND ITS MOTION BEHAVIOR

by

Tianxu Huang

A thesis submitted to Johns Hopkins University in conformity with the requirements for the degree of Master of Science in Engineering

Baltimore, Maryland

May 2019

ABSTRACT

This essay reports on the investigation of the mobilization of a particle initially deposited on a flat plate by a moving liquid-liquid interface. The topic is worth investigation for that the transport of colloidal particles in porous media and moving behaviors when driven by liquid-liquid interface can affect a broad range of industrial process, which are closely related to environment protection and nature resources recovery. Our experimental approach is motivated by results of recent molecular dynamics simulations showing different dynamic regimes during the detachment of a deposited nanoparticle by a moving interface. The main objective of this work is to perform experiments that mimic most of the conditions in the simulations and determine if similar dynamic regimes are observed. A second objective is to investigate the role of surface roughness on the remobilization of deposited particles by a moving fluid interface.

To achieve our objectives, we characterized different particles' motion as a function of the volumetric flow rate. The particles investigated are polymerized ethoxylated trimethylolpropane triacrylate (ETPTA) droplets of either 150μm or 400μm diameter. We control the roughness of the particles by coating different sized silica nanoparticles (150nm, 400nm, 520nm, 700nm) to the particle surface. For the mobilization experiments, particles are placed in glass tube, the oil phase is silicone oil and the aqueous phase is a mixture of water, dimethyl sulfoxide (DMSO) and sodium thiosulfate. By changing the moving speed of the oil-water interface inside the tube,

different particles show different movement characteristics. We observe that particles tend to stay on the surface at low flow rates and start moving when the flow rate increases, followed by detachment at the highest flow rates. At intermediate flow rates, we observe a dynamic regime where the liquid-liquid interface first drags the particle along and then re-deposit the particle further down the microchannel. This regime was not observed in the molecular dynamics simulations. We attempt to obtain a qualitative understanding of the role of the flow rates on particle detachment by performing a force balance on the deposited particle. The force balance suggests that the most important factor on the particle remobilization is the contact angle dependence of the volumetric flow rate.

To have better silica-coated ETPTA particles, the ETPTA's surface property and wettability were studied and during which, an abnormal surface tension increase in water and color change were observed. A brief introduction and explanation of the phenomenon was also introduced in this work.

Committee: Prof. Joelle Frechette (academic advisor, ChemBE)

Prof. Michael A. Bevan (ChemBE)

ACKNOWLEDGEMENTS

I can never find a better opportunity to express my gratitude to my parents for their love and support during my pursuing for my master degree. Thanks to my mom for she always stands behind me whatever difficulties I were facing. I'm also thankful for my dad that it's him who teaches me to stay firm and strong. My family has always been my strongest backup.

Dr. Joelle Frechette, my advisor, is the one I respected the most during my study here. Her knowledge and patience guided me through my master's study. I learnt a lot from her during my research as well as everyday life. I owe a great thank you to Dr. Frechette.

I also want to thank the group members who also are my close friends: Donglee is not only my guider in experiments, but also my first friend here, wish him good luck in his future career life. Nikki and Hanqi helped me a lot in fields related to their research, like surface energy and interfacial tension measurement. Thank for Fu's help during device preparing and experiment procedure improvement. Christian's rich experience in almost every field, especially in chemistry gave me a hand when analyzing ETPTA. Zach and Preetika are so approachable and caring that held parties after weeks' work. Also I want to thank Paul and Anushka's advice on equipment's settings and practical ideas. I couldn't accomplish all I have done without your guys' help.

Finally, I want to thank all my friends who helped me either at school or everyday life here in the U.S. Thanks Zhaonian, Junyan, Yingtian. Life would be really boring

without you here. Also thanks my girlfriend for supporting me for the past two years. You all are treasure of my life.

TABLE OF CONTENTS

LIST OF FIGURES

1. INTRODUCTION

1.1. Significance and objective

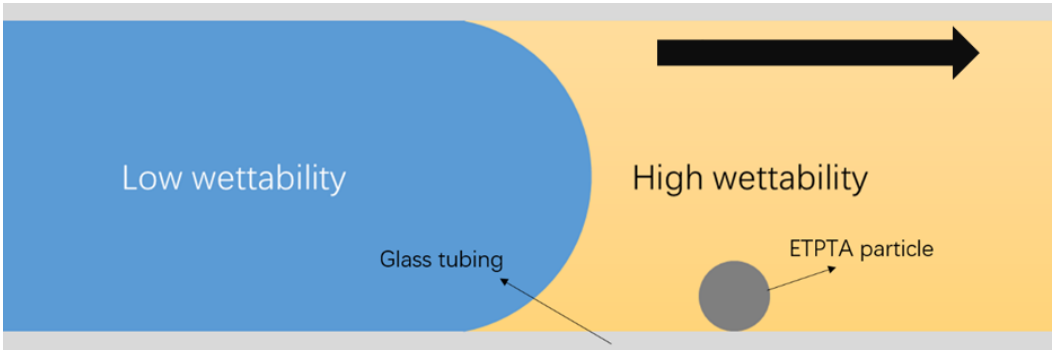

Figure 1. A brief schematic of an ETPTA particle deposited on a plate together with a high-wettability liquid and a low-wettability liquid phase. The arrow stands for fluid direction.

The transport of colloidal particles in porous media can affect a broad range of industrial processes, including particles transport through membrane, water treatment, permeability fluctuation in sandstone reservoirs by fluid injection[1,2]. Understanding the mobilization of a particle that is initially deposited on a fixed plate is of great importance for assessment of colloids' concentration and contaminants' transport in mobile colloids[3]. Static models have been established and progress has been made in understanding the colloid transport in saturated systems[4], but predicting the dynamic behavior of deposited particles remains challenging. Recently, dynamic effects in the mobilization of adsorbed nanoparticles were studied and modifications were applied to existing models[5]. The remobilization of deposited colloidal particles by dynamic liquid-liquid interfaces and moving (three-phase) contact line plays a key role in various fields like groundwater transport in the vadose zone and enhanced oil recovery operations[6,7].

Experimental works were introduced that provide qualitative descriptions of the particle behavior[8], however, only a small number have investigated the how particles are moved by the moving fluid-fluid interface in modeled porous media[9,10] and most of these experiments were performed at a mesoscopic level (i.e., pore-level) and, as a result, particle's remobilization physics is still poorly understood. In recent work molecular dynamics (MD) simulations was employed to investigate the dynamic effects of a deposited particle. The results show rich dynamic regimes between having the particle remaining deposited and being completely remobilized by the moving interface.[5] The objective of this work is to determine if similar dynamic regimes can be observed experimentally. The significance of the work lies in obtaining experimental observations for particle's behavior under similar circumstance and highlight dynamic regimes for the remobilization of individual particles to correspond with results from MD simulations. A second objective is to investigate how surface roughness affects the particle remobilization. Surface roughness is controlled by coating different sized silica based nanoparticles synthesized through Stöber Method[11] to the ETPTA surface as is shown in **Figure 2**.

The experiments are performed using a home-built capillary device to create ETPTA droplets and to coat the droplets with silica nanoparticles. Drop sizes were controlled so that we get monodispersed ETPTA particles with diameter ranging from 150μm to 400μm. By carrying the same experiments with these different particles, we can imitate particle behaviors in real industrial application. To interpret our measurements, we estimated the forces acting on the deposited particles during the

passage of a fluid interface. The results from the force balance are in qualitative agreement with the experimental results.

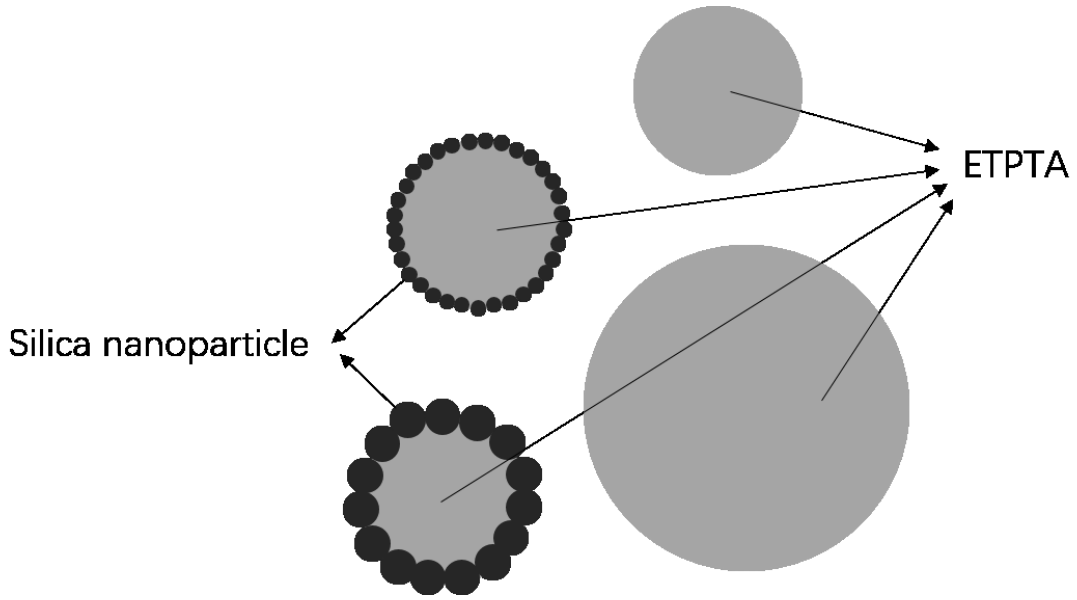

Figure 2. Schematic of the particles investigated, including 150μm and 400μm pure ETPTA particles and 150μm particle with two different sized silica coating.

To create reproducible and stable ETPTA droplets and solution we had to find condition where the interfacial tension of the ETPTA interface was stable and reproducible. Therefore, the final objective of this work was to investigate how ETPTA droplet's surface tension change over time and what caused the turbidity in pure ETPTA drops. During the investigation, an increase of ETPTA's surface tension in water is observed, together with a color change of the droplet as shown in **Figure 3** and **Figure 4**. The coating of silica nanoparticles on ETPTA drops in water strongly depends on surface properties of the particle and liquid interface, especially the wetting property. Also particle's color and transparency strongly affects the observation during the experiment. Through investigating these properties, a suitable aqueous phase's components can be proposed during the fabrication and thus can guarantee the particles we make will have similar properties and suit the following experiments.

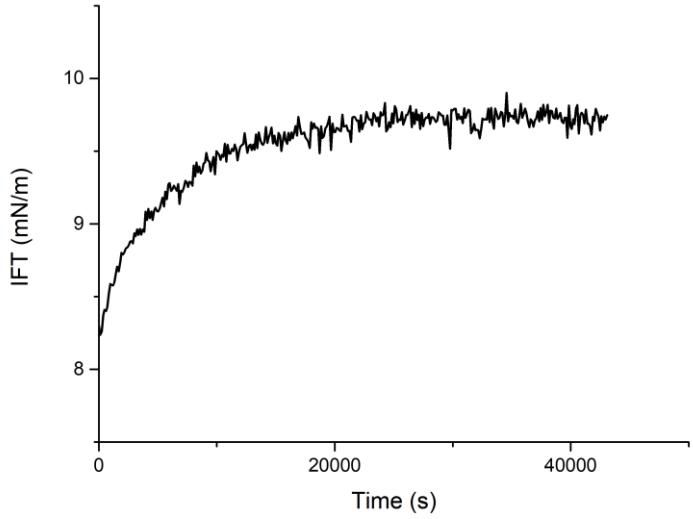

Figure 3. Surface tension change of a ETPTA droplet in water in 12 hours.

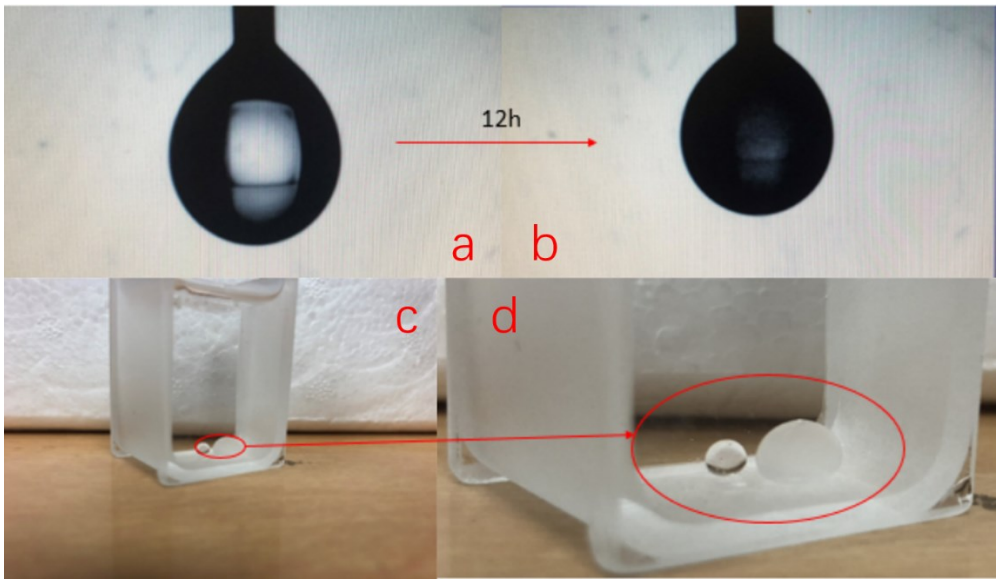

Figure 4. EPTPA droplet's color change after 12 hours. a and c are initial droplet on the screen and b, d are droplets after 12 hours

1.2. Background

In previous work, MD simulations were preformed using the open-source package LAMMPS[12]. Through the MD simulation, a system contains two immiscible liquids confined between two parallel plates and a particle deposited on one of the flat walls was established and videos recording the simulation results can be found in literatures.

As is shown in the **Figure 1** we define an advancing interface, corresponding to the high-wettability liquid displacing the low-wettability one and a receding interface where the low-wettability liquid displacing the high-wettability one according to the flow direction.

By combining the MD simulation with the driving force imposed on the particle, different particle motion behaviors were observed[5]. For small driving force applied, *interfacial pinning* was observed when neither lifting, nor sliding conditions are satisfied, the particle remains attached, or pinned, to the substrate[13]. At larger driving forces, we see that the liquid-liquid interface induces the sliding of the particle along the wall of the tube, this indicates the *stick-slip motion.* During the stick-slip motion, the particle remains at the liquid-liquid interface and resulted in a pinning-sliding motion of the interface itself[14,15]. The last one is *rolling-induced detachment*. For large driving forces, some cases of particle jumping were observed when driven by the receding interface. It is important to recognize that mobilization by sliding or rolling may not necessarily lead to colloid separation from the substrate, which corresponds to the different models[16].

These results documented the role dynamic effect played in the mobilization of absorbed nanoparticles when driven by liquid-liquid interface but lack experimental provement. Existing experiment results also failed to fully agree with theoretical predictions. Particle with different wettability and roughness were not included in previous studies. Which will be talked about in this article.

Ethoxylated trimethylolpropane triacrylate (ETPTA) is used as the base for

particle applied in the experiments. It's a trifunctional monomer widely used in industrial manufacture for its low volatility and fast cure response. It has the property of resistance against weather, chemical, water and abrasion. It mainly shows the properties of acrylic group and follows free radical polymerization process[17]. Photo initiator was applied to start the UV polymerization.

2. THEORY

2.1. Force balance on a deposited particle

2.1.1. Attraction force

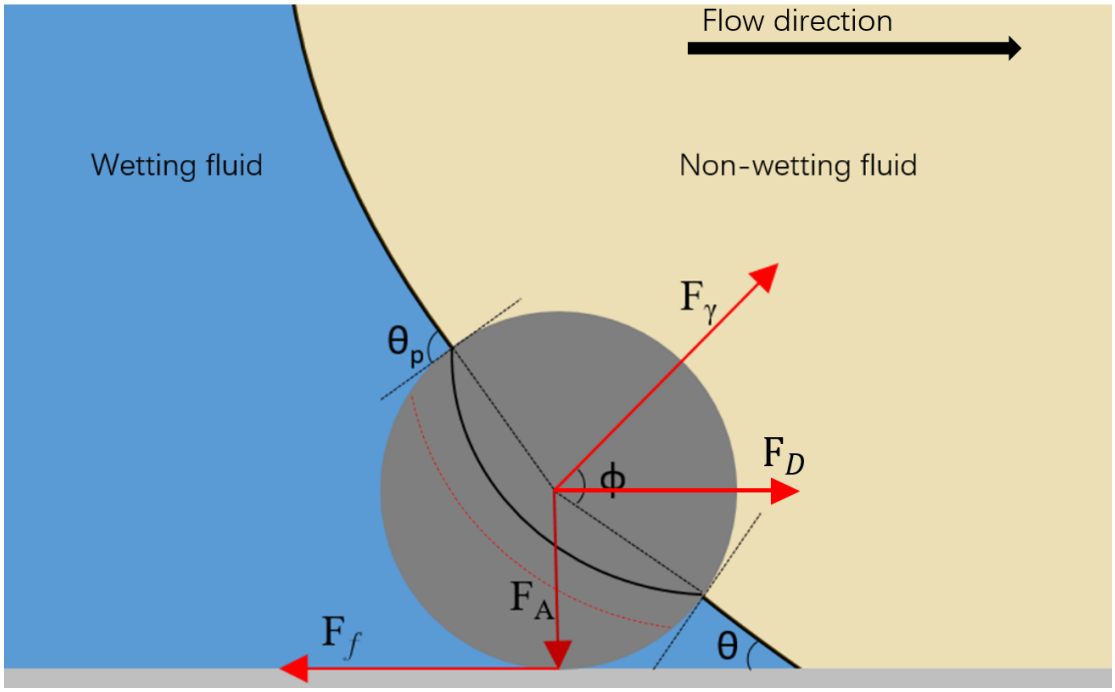

Figure 5. A schematic of the force analysis on a spherical particle attached to a wall. The interface is in contact with the wall with a contact angle θ at with the particle at contact angle θ_p. The view corresponds to a cross-section of the system. Red dashed lines denote the interface equilibrium positions.

Figure 5 is a brief schematic of forces acting on a particle deposited on a glass plate. The particle is affected by forces as follows. Vertically the adhesion force (F_A), gravity force (F_g) and the support by the plate. The particle is also driven by the flow and there is a driving force caused by the flow (F_D), which will be resisted by the friction force of the system (F_f). As the fluid interface passes by both a surface tension force (F_γ) and a force associated by the capillary (Laplace) pressure (F_{Pc}) act on the particle.

For the adhesion force (F_A) here we consider the physicochemical interaction

caused by the combined effect of van der Waals and double layer force[18-21]. We estimate these forces using the Derjaguin–Landau–Verwey–Overbeek theory (DLVO) theory[22].To make this problem tractable we make a series of assumptions (discussed below) to simplify the description of the interaction between the particle and the surface.

We follow closely the approach from Israelachvili's *Intermolecular and surface forces*[21]. We assume additivity of the interaction energy between a molecule and planar surface made up of like molecules[21,23]. Therefore, the net van der Waals interaction energy for a molecule at distance D from a flat plate can be expressed as,

$$\omega(D) = -2\pi C\rho_1 \int_{z=D}^{z=\infty} dz \int_{x=0}^{x=\infty} \frac{xdx}{(z^2+x^2)^3} = -\frac{\pi C\rho_1}{6D^3} \quad (2)$$

where $\omega(D)$ is the interaction energy between the molecule and the surface, ρ_1 is the number density of the surface, z is the axis perpendicular with the surface and passes across the molecule and x is the axis perpendicular with z axis. As a result, for a large sphere with radius R, the interaction can be expressed as

$$\omega(D) = -\frac{2\pi C\rho_1\rho_2}{12} \int_{z=0}^{z=2R} \frac{(2R-z)zdz}{(D+z)^3} \approx \frac{\pi^2 C\rho_1\rho_2 R}{6D} \quad (3)$$

where ρ_2 is the number density of the sphere. According to Derjaguin approximation, this can be expressed as:

$$\omega(D) = -\frac{AR}{6D} \quad , \quad (4)$$

where A stands for the Hamaker constant, given as[21,24]

$$A = \pi^2 C\rho_1\rho_2 \quad . \quad (4)$$

So the force can be expressed as

$$F = -\frac{dW}{dD} = -\frac{AR}{6D^2} \quad (5)$$

As for the double layer force, this mainly occurs between charged objects and

results in the development of a wall surface potential which will cause a rearrangement of ions in the surrounding solution. This force should be repulsive for two similarly charged objects and decrease rapidly at larger distance. But as for unequally charged objects at short distance the interactions can also be attractive. The region near the surface of enhanced counterion concentration is called the electrical double layer (EDL). The EDL can be approximated by a sub-division into two regions. Ions in the region closest to the charged wall surface are strongly bound to the surface. This immobile layer is called the Stern or Helmholtz layer. The thickness of the diffuse electric double layer is known as the Debye screening length[21]:

$$k = \sqrt{\sum_i \frac{\rho_{\infty i} e^2 z_i^2}{\varepsilon_r \varepsilon_0 k_B T}} \quad , \tag{6}$$

with unit of m^{-1} ,where $\rho_{\infty i}$ is the number density of ion i in bulk, z is the valency of the ion, ε_r is the relative static permittivity and ε_0 is the vacuum permittivity, k_B is the Boltzmann constant. Thus the repulsive free energy between can be expressed as:

$$W = RZe^{-kD} \quad , \tag{7}$$

where *Z* here is defined by:

$$Z = 64\pi\varepsilon_0\varepsilon(k_B/e)^2 tanh^2(ze\psi_0/4k_BT).\text{J m}^{-1} \text{ or N} \tag{8}$$

So the double layer force between a sphere and wall can be expressed by:

$$F = -\frac{dW}{dD} = kRZe^{-kD} \quad , \tag{9}$$

Where ψ_0 is the surface potential. By combining the van der Waals interaction energy and the double layer interaction energy, the interaction between two particles or two surfaces in a liquid can be expressed as:

$$W(D) = W(D)_A + W(D)_R \quad , \tag{10}$$

where $W(D)_A$ is the attractive interaction energy from van der Waals interaction and $W(D)_R$ is due to repulsive interaction energy.

2.1.2. Surface tension force

When the liquid-liquid interface moves past the particle due to the flow of the liquid, the three-phase contact line moves along the particle surface, leading to a surface tension force F_γ. In addition, the presence of a liquid-liquid interface leads to a capillary pressure force, F_{Pc}, which originates from the Laplace pressure difference between the two liquids due to the (net) curvature of the liquid-liquid interface[5]. As for the surface tension force, θ_p is the dynamic contact angle on the particle surface, φ is the angle that determine the position of the contact line, which is also called the filling angle[25]. The filling angle goes from 0° to 180° when the receding interface moves past the particle and from 180° to 0° for an advancing interface. Sometimes the supplementary angle $\pi - \varphi$ is also used as the filling angle. The red dashed line in **Figure 5** stands for the position where equilibrium is reached and F_γ=0 ($\varphi=\theta_p$) and a flat surface is reached[5]. The surface tension for a flat interface is described as [13]:

$$F_\gamma = 2\pi r\gamma sin\varphi \sin(\theta_p - \varphi) \tag{11}$$

Since the surface tension force will assume two magnitude maxima, F_γ reaches its maximum value twice for both $\varphi = \theta_p/2$ $(\varphi < \theta_p)$ and $\varphi = (\theta_p + \pi)/2$ $(\varphi > \theta_p)$. How surface tension affects the particle also depends on the dynamic contact angle with the plate and the particle surface which are indicated by θ and θ_p. Then the

horizontal and vertical component of maximum surface tension can be expressed as:

$For\ \ \varphi < \theta_p$:

$$F_\gamma^y = 2\pi r\gamma sin^2\left(\theta_p/2\right)sin\theta \tag{12}$$

$$F_\gamma^z = 2\pi r\gamma sin^2\left(\theta_p/2\right)cos\theta \tag{13}$$

$For\ \ \varphi > \theta_p$:

$$F_\gamma^y = -2\pi r\gamma sin^2\left(\theta_p/2+\pi\right)sin\theta \tag{14}$$

$$F_\gamma^z = -2\pi r\gamma sin^2\left(\theta_p/2+\pi\right)cos\theta \tag{15}$$

The particle will experience the maximum surface tension twice in different directions as the liquid-liquid interface passes by the particle, and this process is reversed for receding interface and advancing interface. Also θ_p will affect the direction of the surface tension force.

We consider here a channel with height *H*, the curvature away from the particle can be estimated as :

$$r_c = H/(2cos\theta) \quad . \tag{16}$$

As a result, the capillary pressure force can be estimated as :

$$F_{pc} = \pi R^2 sin^2\varphi\Delta p = \pi R^2 sin^2\varphi\gamma 2cos\theta/H \ , \tag{17}$$

where the Laplace equation:

$$\Delta p = \gamma/r_c \qquad , \tag{18}$$

is applied to equation (17).

2.1.3. Additional forces

Other forces include the dynamic driving force from the flow, gravitational force

and the friction force that resists sliding. For a sphere initially deposited on a flat plate in an imposed shear flow the driving force can be calculated as[26 27]:

$$F_D = 1.701(6\pi\mu G r^2) \quad , \tag{19}$$

where μ is the fluid viscosity, r is the radius of the sphere and G is the shear rate. Normally fluid velocity parallel to the plate at distance z is considered as

$$v_y = Gz \tag{20}$$

The interactions between the particle and the plate also include the gravity:

$$F_g = (\rho_1 - \rho_2)gV \quad , \tag{21}$$

where F_g is the gravitational force, g is the gravitational acceleration, ρ_1 and ρ_2 are density of the liquid phase and the particle respectively, and V is the particle volume. During the moving of the interface, the particle is gradually immersed in two different liquid phases and there is a density difference between the two phases. However, this can be considered negligible since it's several orders of magnitude less than F_A especially when the aqueous phase's density is maintained similar to particle' density.

2.2. Silica nanoparticle synthesis

The silica nanoparticles we use are synthesized through Stöber method[11]. Since its first proposed, modifications have been adapted to traditional Stöber method to synthesize particles from less than 100nm to few microns[28,29] in diameter. Typically, there is a one-step Stöber method and a modified two-step method[30] to target different sizes, and the one-step method is employed in this study. With this method, silicon

alkoxide, usually tetraethylorthosilicate (TEOS) is hydrolyzed in alcohol in the presence of a basic catalyst, mainly ammonia[31,32]following:

$$\mathrm{Si(OEt)_4 + H_2O \rightarrow Si(OEt)_3OH + EtOH} \quad (22)$$

$$\mathrm{Si(OEt)_4 + 2H_2O \rightarrow Si(OEt)_3(OH)_2 + 2EtOH} \quad . \quad (23)$$

The reaction produces ethanol and a mixture of ethoxysilanols, which will condense with either TEOS or other silanol with loss of alcohol or water. The additional reactions are:

$$\mathrm{2Si(OEt)_3OH \rightarrow (EtO)_3 - O - Si(OEt)_3 + H_2O} \quad , \quad (24)$$

$$\mathrm{Si(OEt)_3OH + Si(OEt)_4 \rightarrow (EtO)_3 - O - Si(OEt)_3 + EtOH} \quad , \quad (25)$$

$$\mathrm{Si(OEt)_3OH + Si(OEt)_3(OH)_2 \rightarrow (EtO)_3 - O - Si(OEt)_3 + H_2O} \quad . \quad (26)$$

Further hydrolysis of the ethoxy groups and subsequent condensation leads to crosslinking. It is a one-step process as the hydrolysis and condensation reactions occur simultaneously in a single reaction vessel.

2.3. ETPTA droplets coated with silica nanoparticles

To vary the surface roughness of the deposited particles, silica nanoparticles were coated on ETPTA droplets' surface and then polymerized to obtain a solid particle. To have those particles form a homogeneous monolayer on the droplet surface, we utilized properties of Pickering emulsion. A Pickering emulsion is an emulsion that is stabilized by solid particles (for example colloidal silica) which adsorb onto the interface between the two phases[33]. If the contact angle of the interface on the particle is approximately 90°, which means the particle is partially wettable by both liquids, and as a result liquids

bind better to the droplet surface.

The stabilization energy is given by:

$$\Delta E = \pi r^2 \gamma_{OW}(1 - |cos\theta_{OW}|)^2 \ , \quad (27)$$

where r is the particle radius, γ_{OW} is the interfacial tension and θ_{OW} is the contact angle at the interface.

2.4. Formation of water droplets in oil phase

Color change in oil that is in contact with water resulted from nucleation has been reported before[34]. Ouzo effect was reported to cause the effect but it is not sufficient for all cases[35]. Yang's group observed spontaneous formation of water drops on octadecyltrichlorosilane (OTS)-treated glass[34]. In their experiments, droplets grew to 30-40μm in diameter in 10 days and tended to disappear with further incubation. After that new droplets were observed to form and grow again to reach similar dimensions. Similar observations were reported within liquid phase but not only liquid impregnated surfaces[36]. The authors considered the presence of a nucleation energy barrier related to the wettability between the liquids and also the solid surface. By adding salt (NaCl) the nucleation velocity and drop size changed and no water drop formation was observed at high salt concentration. Two factor were considered key to the nucleation to occur on solid surface: the charge density of the solid substrate needs to be high and macroscopic contact angles of the water droplets on the surface need to be sufficiently large to cause dewetting of water under the oil[35]. Regimes for nucleation in bulk liquid phase and physics behind the phenomenon was also reported [35].

3. METHODS

3.1. Materials, chemicals, equipment and instruments

Table 1. Materials, chemicals, equipment and instruments applied in the experiments

Chemicals and materials	Distributor
Ethanol alcohol	Fisher Chemical (PA)
Ammonia solution	Fisher Chemical (PA)
Deionized (DI) water	In-house Milli-Q Academic water purification system
Isopropanol	OmniSolv® from VWR International, LLC.
Toluene	OmniSolv® from VWR International, LLC.
Acetone	Fisher Chemical (PA)
Hydrogen peroxide	Fisher Chemical (PA)
Sulfuric acid (98%)	J.T.Baker® from Avantor (PA)
Trimethylolpropane ethoxylate triacrylate (ETPTA) Mn ~ 428	Sigma-Aldrich (PA)
Poly(ethyleneglycol)-block-poly(propyleneglycol)-block-poly(ethylene glycol) (Synperonic® F 108)	Sigma-Aldrich (PA)
(3-Aminopropyl)triethoxysilane (APTES)	Gelest (PA)
Photoinitiator (2-Hydroxy-2-methylpropiophenone)	Sigma-Aldrich (PA)

Dimethyl sulfoxide (DMSO)	Fisher Chemical (PA)
Polydimethylsiloxane, trimethylsiloxy terminated (silicone oil), 2 cSt	Gelest (PA)
Rhodamine B	Sigma-Aldrich (PA)
Tetraethyl orthosilicate (TEOS)	Sigma-Aldrich
Sodium thiosulfate	Fisher Chemical (PA)
Sodium chloride	Fisher Chemical (PA)

Equipment and instruments	Brand
BD Intramedic™ PE Tubing (0.034in ID)	Fisher Scientific (MA)
Extreme-Temperature Teflon® PTFE Semi-Clear Tubing for Chemicals, 1/32" ID	Mcmaster-Carr (NJ)
Needle with Luer Lock Connection (1/2" Needle Length, 21 Gauge)	Mcmaster-Carr (NJ)
Square-Profile Oil-Resistant Buna-N O-Rings	Mcmaster-Carr (NJ)
Glass cylindrical capillary (0.2mm ID)	Vitrocom (NJ)
Square glass tube (0.4mm ID)	Vitrocom (NJ)
Glass tube (2mm×2mm)	Vitrocom (NJ)
Silastic laboratory tubing (1.6mm ID)	Dow Corning (MI)
Programmable syringe pump PHD2000	Harvard Apparatus (MA)
Programmable syringe pump Pump 11 Elite	Harvard Apparatus (MA)
Zetasizer Nano ZS for Dynamic Light	Malvern Panalytical (UK)

Scattering (DLS)	
Microscope BH2-UMA	Olympus (JP)
UV light UVP UVGL-55	Analytikjena (Germany)
Stringray F125B camera	Allied Vision (Germany)
B/W camera	APPRO (Taiwan)
75mm×25mm×1mm glass slide	Fisher Scientific (MA)
22mm×22mm-1 glass cover	Fisher Scientific (MA)
3ml syringe	BD (NJ)
60ml syringe	BD (NJ)
Software	
Zetasizer family software	
TSview7	
Fta32	
Vimba Viewer	
OBS studio	

3.2. Synthesis and Characterization of Silica Nanoparticles

3.2.1. Synthesis process

The nanoparticle's target diameter is given by the empirical formula:

$$d = A \cdot \left(c_{H_2O}\right)^2 \cdot \exp(-B \cdot \left(c_{H_2O}\right)^{1/2}) \quad , \tag{28}$$

$$A = (c_{TEOS})^2 \cdot (82 + 151 \cdot c_{Ammo} + 1200 \cdot (c_{Ammo})^2 - 366 \cdot (c_{Ammo})^3) \quad , \tag{29}$$

$$B = 1.05 + 0.523 \cdot c_{Ammo}. - 0.128 \cdot (c_{Ammo})^2 \quad , \qquad (30)$$

where d is the target diameter, c_{H_2O} is water concentration, c_{Ammo} is the ammonia concentration and c_{TEOS} is TOES concentration of the mixture.

During the synthesis process, first we need to clean both the stir rod and glass vial using isopropanol alcohol (IPA), then blow with air. We then add desired amount of water to the volumetric cylinder using a pipette and then pour water to the glass vial. After that ammonia solution was added to the vial (when extracting the ammonia, pump up and down multiple times to wet the wall of the pipette, it will prevent ammonia from dripping out from the tip). 200 proof ethanol was added to the vial up to desired target volume by pouring directly. We then pipette up and down with the glass pipette to mix the contents of the continuous phase. We then place the vial on stir plate and stir at ~300 for around 5 minutes. After we achieve uniform mixing we add TEOS drop by drop slowly to the glass vial using 200ml pipette while stirring. Finally, we make sure the vial is capped tightly and allow solution to stir and react for 24 hours.

After the reaction is complete, we need to clean out the excess chemicals in the solution. First we need to separate the particle solution into centrifuge tubes. We use sedimentation velocity to determine centrifuge speed and time, longer centrifuge time and higher speed was applied for smaller particles. We program the tabletop centrifuge with the chosen speed and time. After the centrifugation, we remove and dispose of supernatant, then re-suspend the nanoparticles in ethanol using vortex and sonicator. We repeat these steps in water for at least 5 times and switch to ethanol until the pellet

is difficult to see. Particle solution was concentrated to half of the tubes after every other wash, and was finally concentrated to two tubes.

3.2.2. Characterization and yield of nanoparticles

We need to know the concentration to keep our reaction conditions the same. First weigh a 1.5 mL microcentrifuge tube and record the weight up to 4 decimal places, then add 100 μl of particle solution to the tube. We then place the tube inside a 20 ml vial and keep the cap open and put the entire container on a stir plate. We set the plate temperature to 70°C and leave for a few hours until all the ethanol evaporated. After full evaporation, we weigh the tube and dry the particles and subtract from initial weight to get the particle weight. The difference (in mg) in mass is the particle weight percent (ex. 7.5 mg of dry particles means we have a 7.5 wt.% particle solution). We then label the particle solution with the particle material, size, concentration, date and store the sample in the refrigerator.

The particle size was measured by Dynamic Light Scattering (DLS). The particle solution was diluted 1000 times in the PMMA cuvette for DLS measurement. Zetasizer Nano ZS and associated software were used in the test. For the software settings, the settle time was set to 120s, and we input the refractive indices of water and silica. We perform three runs to obtain results for which the PDI is less than 0.3. We use this criterion to determine if the particles can be considered as usable.

3.3. Preparation and characterization of silica-coated ETPTA droplets

3.3.1. Device preparation

A handcrafted capillary device was utilized for preparing silica-coated ETPTA droplets. First we mix 5ml toluene and 10μl APTES in the 20ml glass vial and sonicate for 5 minutes. Then we put the 0.4mm ID glass tube in the vial and tilt the vial to let the mixture rise to the top by capillary force and keep the vial in the fume hood for another 5 minutes with the cap opened. The capillary is washed with acetone and DI water after the treatment and is attached to the PE tubing, which will work as the outlet tubing of the device and glued to a glass slide. Then we pre-washed 0.2mm ID capillary with one end narrowed with fire is inserted to the glass tube and the joint is covered with the needle as well as the other end of the capillary. The needles are connected to the syringe using the Teflon® PTFE tubing and work as the inlet of the device. **Figure 6** is a sample of the capillary device.

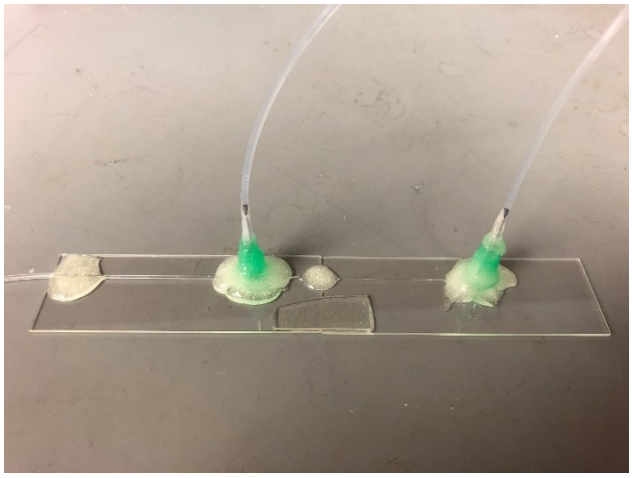

Figure 6. A sample of the glass capillary device

3.3.2. Droplet formation

We take 1.5ml ETPTA and mix it with the proper amount of particle solution (or only ETPTA for pure ETPTA droplets' preparation), we then keep the vial in a vacuum oven with cap open overnight at 70℃ and evaporate all ethanol to prepare 10wt. % particle's ETPTA solution. We then add 1wt. % photoinitiator to the mixture and wrap the vial with aluminum foil. We then prepare 1wt. % F108 block copolymer surfactant solution and 1M NaCl solution and equal amount of which are mixed to prepare the aqueous phase. We introduce the aqueous phase with a 60ml syringe and introduce the ETPTA solution with a 3ml syringe. We connect the 60ml syringe to the inlet at the joint and the 3ml one to the needle at the end. ETPTA solution is pumped into the capillary at a flowrate of 5µl/min. Then water is pumped into the glass tube at 200µl/min volumetric flowrate to prepare 400µm diameter droplet and 1000µl/min for 150µm droplets. **Figure 7** gives a graphical representation of the process. Observe the capillaries' narrowed end with 10× microscope. We collect the droplets in a 20ml vial. The emulsion droplets were photopolymerized by exposure to UV light for 30 seconds, then we let them rest one-hour in the dark, followed by a with water until no froth is observed. Finally, we mark the vial with name and date and store properly.

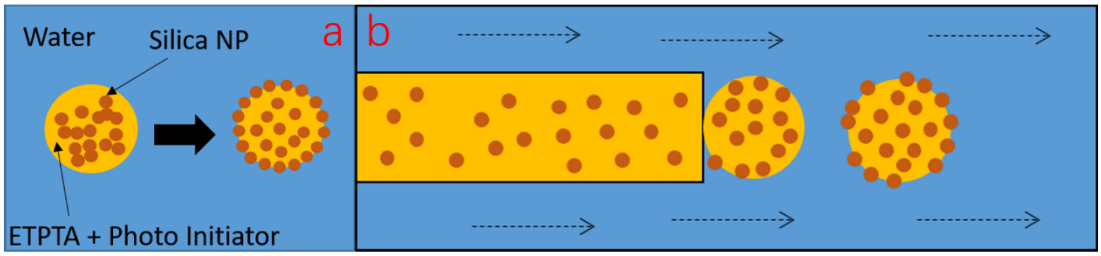

Figure 7. (a) Illustration of the formation of Pickering emulsion in a capillary device. The silica nanoparticles dispersed in ETPTA will form a homogenous layer at the oil-

water interface when in contact with water. **(b)** Illustrations of the multiphase flow in the capillary device.

3.4. Particle motion and contact angle measurement

3.4.1. Device preparation

We cut the 2mm×2mm glass tube into 5cm length pieces, then mix the sulfuric acid and hydrogen peroxide (volume ratio 3 to 1) in a beaker to prepare piranha solution. We keep the tubes in piranha for one hour until no bubbles are observed on tube surface. Then take out the tubes carefully and wash them with water. Then we take one large ETPTA particle with capillary and transfer it to the tube. In the process we make sure the particle is not stuck to the tube's side walls and not trapped at the edge. After that, we attach the silicon tubing to the glass tube and glue the whole thing to the glass slide with epoxy. Finally, we connect one end of the device to a syringe and the other end to the container.

3.4.2. Observation of liquid-liquid interface motion past a spherical particle

We take 2.0cSt silicone oil as the oil phase of the system. The aqueous phase is a mixture of water, dimethyl sulfoxide and sodium thiosulfate (56.7wt.% water, 36.5wt.% DMSO, 6.8wt.% sodium thiosulfate for pure ETPTA particles and 50.7wt.% water, 32.6wt.% DMSO, 16.7wt.% sodium thiosulfate for silica nanoparticle-coated droplets). DMSO is added to match the refractive index with silicone oil and final viscosity is 2.2cSt. We add traces of Rhodamine B to the aqueous phase to have a better view under

the camera to tell the interface's position, then vibrate to mix well. Then, salt is added to the aqueous phase to match the density with ETPTA particles (1.11g ml-1 for pure ETPTA particles and 1.21g ml-1 for silica-coated ETPTA particles). The viscosity of the aqueous phase is 2.2 cSt to minimize the difference between phases. We position the glass tube horizontally in front of a camera to record the motion of the liquid interface and that of the particle. The oil phase is pumped into the glass tube initially, followed by the aqueous phase. The volumetric flow rates are varied between 1 and 5000 $\mu l\ min^{-1}$ both for infuse and refill using a syringe pump.

3.5. ETPTA's surface tension increase and color change study.

3.5.1. Experiment on surface tension change

To find out what affects the ETPTA's surface tension change in water, several assumptions were made, including it's the material's natural property, temperature effect, or polymerization. To tell if it's ETPTA's unique characteristic, it's surface tension in air is measured. To eliminate the temperature effect, a modification to the Pendant drop tensiometer is applied, by switching the bulb shelter with one covered with insulation tape, as shown in **Figure 8**. To minimize the influence of polymerization, another modification is applied to the system. A UV filter is set and a shelter covered with aluminum foil is made to block UV light. The experiment is carried out under total darkness. **Figure 9** shows the schematic of the new system. All measurement last for 12 hours and results are compared to show is the assumptions are the causes for the

tension change. Results are also compared to reported values to determine applicable value for this study.

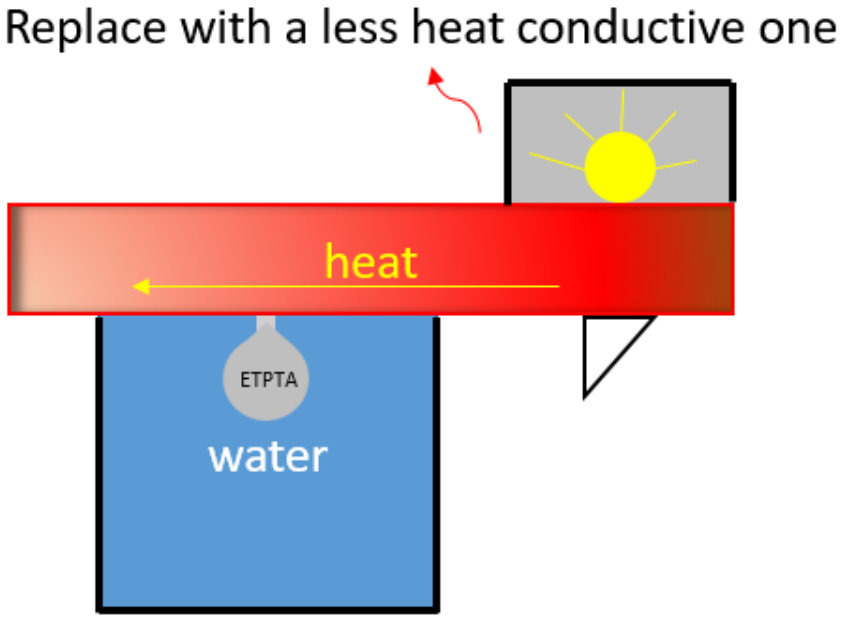

Figure 8. Schematic of the modification to the instrument to minimize the influence of temperature change of the ETPTA droplet. Temperature is 8°C lower than before the modification.

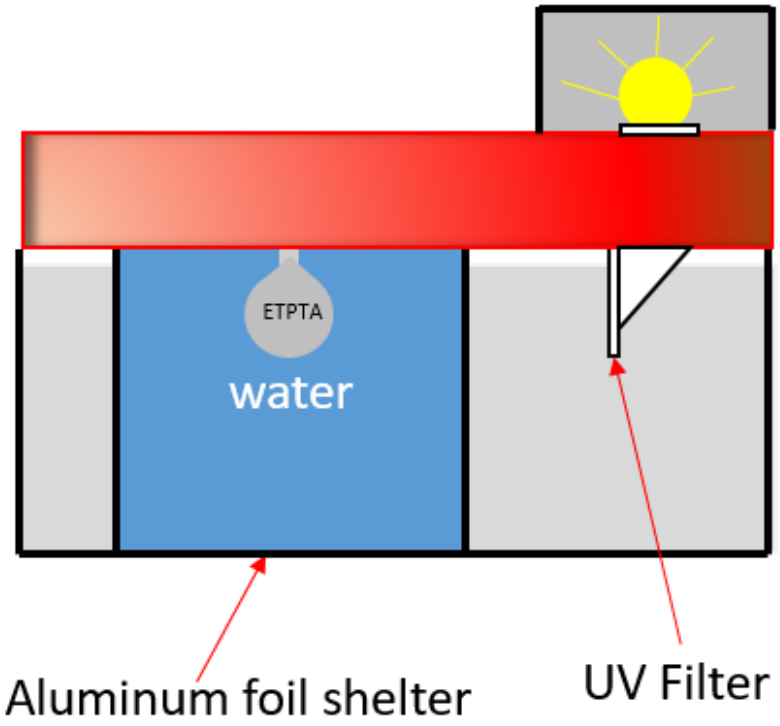

Figure 9. Schematic of the modification to the instrument to minimize the influence of

UV light to the ETPTA droplet. UV filter from Canon® and aluminum foil are used to shelter the droplet from polymerization. During the experiment, all lights were turned off.

3.5.2. Experiment on water nucleation in ETPTA

During the surface tension measurement, ETPTA droplets get turbid while they should remain transparent. A device is prepared to observe if the turbidity is caused by the nucleation of small water droplets within the oil phase, analogous to observations by other researchers[34]. For these measurements, we use a rubber O-ring on a glass slide fixed by epoxy to form a well. We use pipette to place a tiny ETPTA drop on the slide, then fill the O-ring with water. We then place the glass cover on the convex liquid surface to seal the well. The preparation is shown in **Figure 10**. We observe the device with a microscope to see if there is drop formation. We perform similar additional experiments but in a PMMA cuvette to investigate the role of surface charge on the nucleation process.[36] Finally, we repeat the experiments but with different amount of salt (NaCl) added to the aqueous phase to investigate if the presence of salt limits nucleation of water in ETPTA[36].

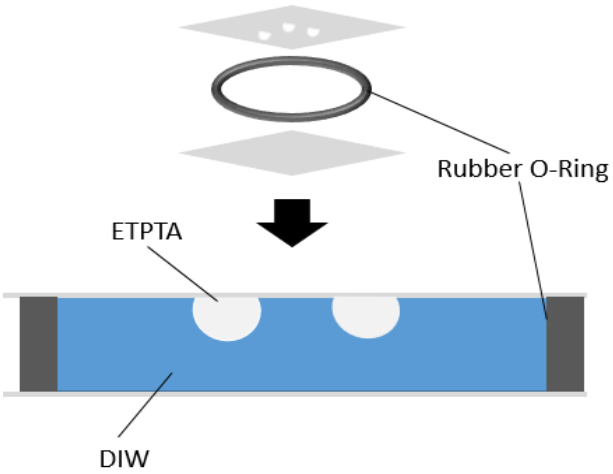

Figure 10. Preparation of the O-ring-well device

4. RESULTS AND DISCUSSION

4.1. Results and discussion for particle motion tests

4.1.1. Observations of particle motion

As is shown in the **Figure 11**, different particle behaviors have been observed during the experiment. To follow the terminology with the one in previous study[5], here I introduce particle behaviors as follows: Interfacial pinning, Stick-slip motion, Stick-slip motion with horizontal detachment and Stick-slip motion with vertical detachment.

Interfacial pinning. Interfacial pinning indicates when the interface passes by the deposited particle and the particle remains at its initial position and is not affected by the interface. Particles might have minimal displacement when first in contact with the interface but will remain static afterwards as if the particle is pinned to the glass tubing.

Stick-slip motion. For higher flow rate, particles will have stick-slip motion, for which particle is driven by the interface. During the stick-slip motion, the deposited particle is trapped at the interface when interface moves past the particle and is moved by it. However, a pinning-sliding intermittent motion of the particle is observed during the axial movement. The particle will not leave the liquid-liquid interface during the stick-slip motion

Stick-slip motion with horizontal detachment. Another particle behavior is observed at even higher flowrates. During the process, the deposited particle is moved by the interface, in a fashion similar as for the stick-slip motion, but then the particle slides with the interface. After a while the interface passes the particle and the particle

is re-deposited on the solid surface in either liquid phase (aqueous phase while driven by a receding interface and oil phase for an advancing interface in our case). The particle keeps sliding on the plate and there is no detachment with the plate.

Stick-slip motion with vertical detachment. The last regime also starts from stick-slip motion, but is only observed at the highest flow rate. Here, when the interface reaches the particle at a very high speed, the particle will not only be moved by the interface in a horizontal direction, but will also be lifted by the interface. Stick-slip motion with vertical detachment is only observed occasionally at high flow rate region (1000 ~ 5000μl/min).

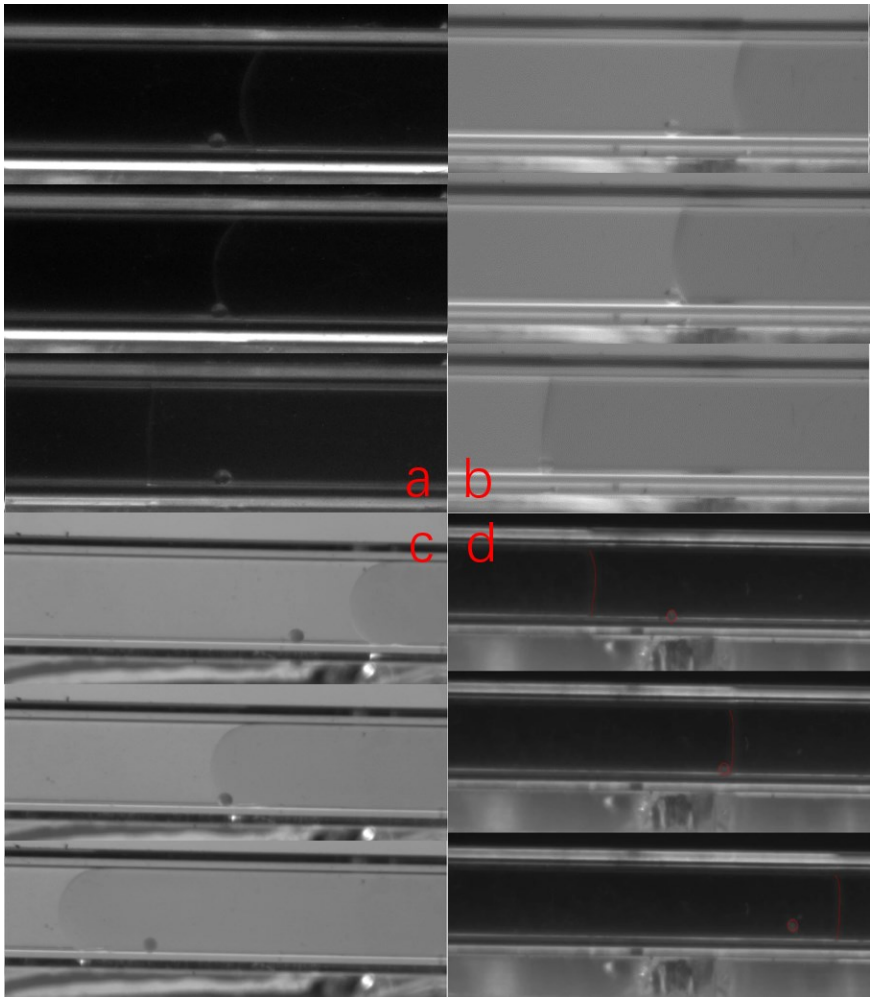

Figure 11. Images for all four particle behaviors observed. **(a)** stands for *interfacial pinning*, while the particle remains static when the interface moves past it. **(b)** is *stick-*

slip motion. The particle is affected by the interface and moves with the interface alongside the wall. No detachment is observed. **(c)** is for *stick-slip motion with horizontal detachment.* The particle is affected by the interface and moves with the interface for a while, then the interface moves past the particle and the particle re-deposits on the surface. **(d)** is a *stick-slip motion with vertical detachment*. When the interface reaches the particle at high velocity, the particle is lifted by the interface and jump into the bulk liquid phase.

The observation results are shown in **Figure 12, 13, 14 and 15**, where different particles are identified by r_1/r_2, when r_1 is the diameter of silica nanoparticle and r_2 is the diameter of the ETPTA particle.

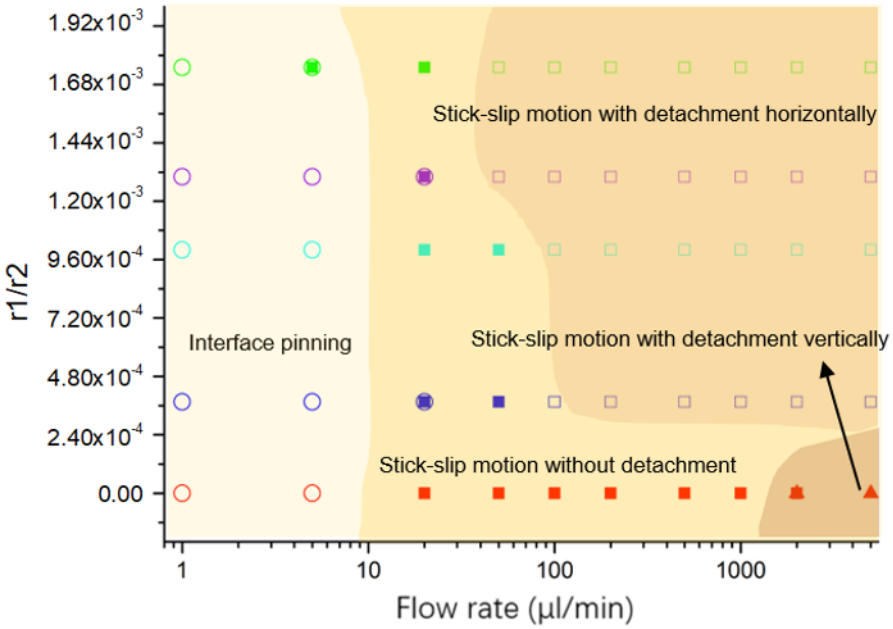

Figure 12. 400μm particles' behaviors regime when driven by receding interface. Circles indicate interface pinning, squares are for stick-slip motion, triangles for stick-slip motion vertical detachment. Solids symbols mean no horizontal detachment observed and open symbols indicate droplet leaves the interface during the movement. Two symbols together means both behaviors have been observed. (Note that boundaries between regions are just for classification but not exact values where change happens)

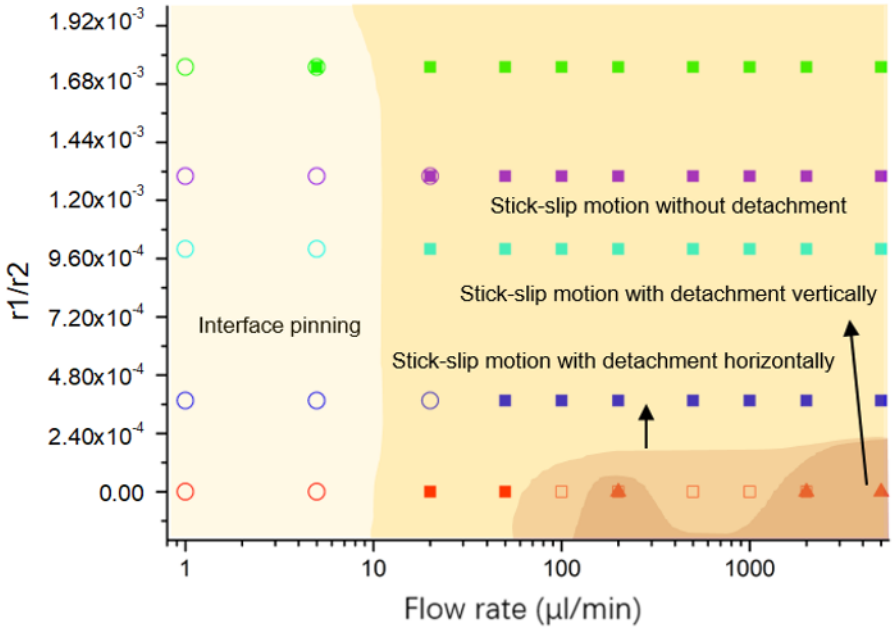

Figure 13. 400μm particles' behaviors regime when carried by advancing interface. Circles indicate interface pinning, squares are for stick-slip motion, triangles for stick-slip motion vertical detachment. Solids symbols mean no horizontal detachment observed and open symbols indicate droplet leaves the interface during the movement. Two symbols together means both behaviors have been observed. (Note that boundaries between regions are just for classification but not exact values where change happens)

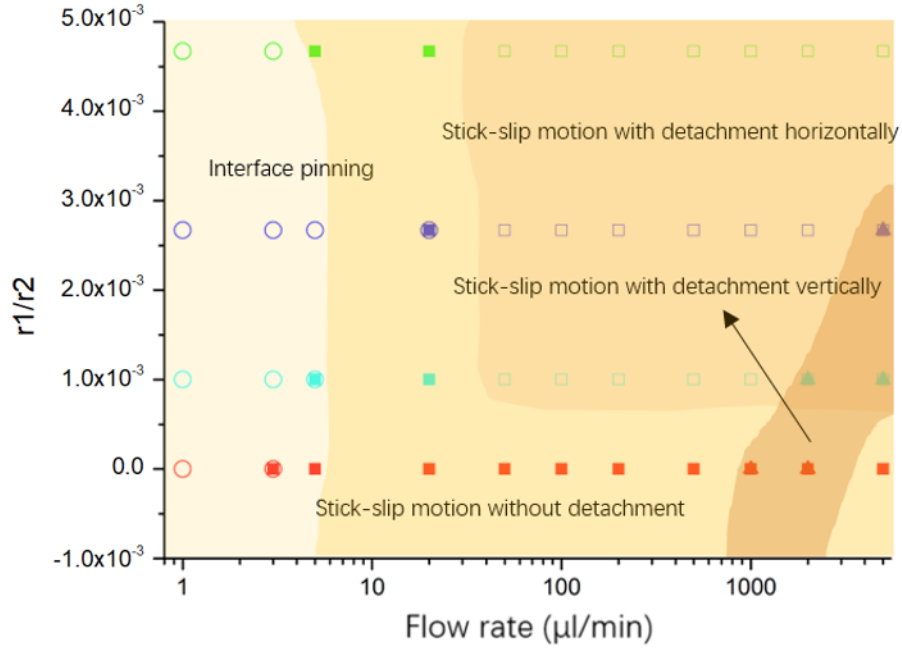

Figure 14. 150μm particles' behaviors regime when carried by receding interface. For both figures, circles indicate interface pinning, squares are for stick-slip motion,

triangles for stick-slip motion vertical detachment. Solids symbols mean no horizontal detachment observed and open symbols indicate droplet leaves the interface during the movement. Two symbols together means both behaviors have been observed. (Note that boundaries between regions are just for classification but not exact values where change happens).

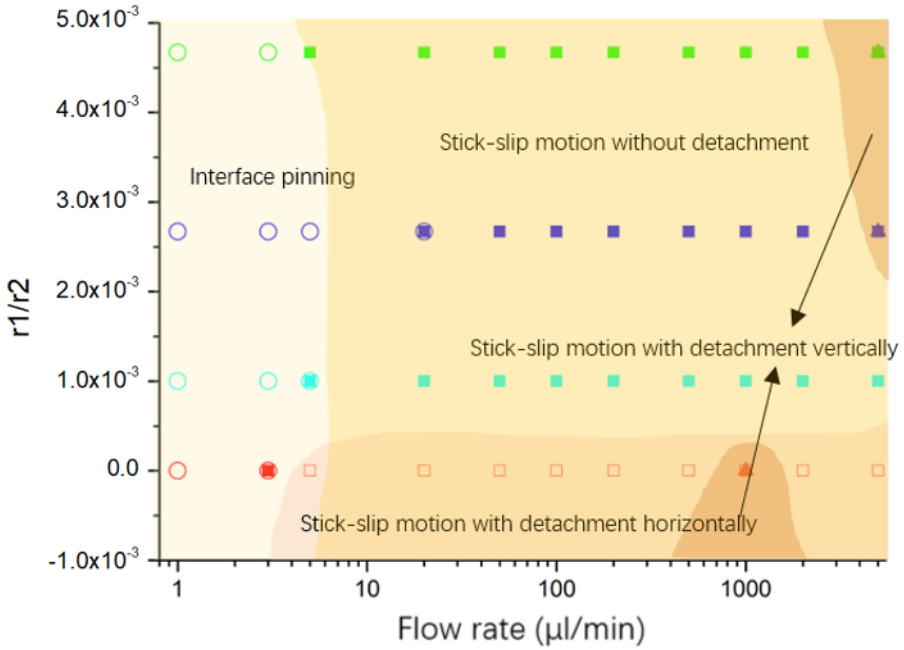

Figure 15. 150μm particles carried by the advancing interface. For both figures, circles indicate interface pinning, squares are for stick-slip motion, triangles for stick-slip motion vertical detachment. Solids symbols mean no horizontal detachment observed and open symbols indicate droplet leaves the interface during the movement. Two symbols together means both behaviors have been observed. (Note that boundaries between regions are just for classification but not exact values where change happens).

As is shown in **Figure12, Figure 13, Figure14 and Figure15**, different particle behaviors have been marked with different symbols. Also regions where same motion type occurs most frequently are indicated with the same color (Note that boundaries between regions are just for classification but not exact values where change happens). Below we discuss the experimental observations from the dynamic regime maps.

The first is that for both 150μm and 400μm particles, particles with and without silica coating have different motion behaviors. Pure ETPTA droplets have horizontal detachment at a flow rate of around 20μl/m to 1000μl/m when driven by the advancing

interface but do not have stick-slip motion with horizontal detachment when contacted by a receding interface. However, particles that have silica nanoparticles on the surface exhibit the opposite pattern while detachment happens when driven by the receding interface. But for both kinds of particles, motion behavior will change from interfacial pinning to stick-slip motion when flow rate increases when driven by the receding interface as well as the advancing interface. For silica-coated particles at receding interface and pure ETPTA particles at advancing interface, stick-slip motion will change to stick-slip motion with detachment horizontally if the flow rate keeps increasing.

Vertical detachment mainly happens at high flow rate region (1000 ~ 5000 μl/min) and no vertical detachment is observed for 400 μm silica-coated particles only pure ETPTA particles. Also, as shown in **Figure 16**, for both 150 μm pure ETPTA particles and 150 μm particles coated with 150 nm silica nanoparticles, vertical detachment was observed. Similar observations have been recorded for other combinations. Here we come to the conclusion that it is easier for vertical detachment to happen when the droplet has a smaller diameter and without silica particle coating. Despite vertical detachment, different sized particles with the same nanoparticle coating follows similar patterns when the flow rate is increased.

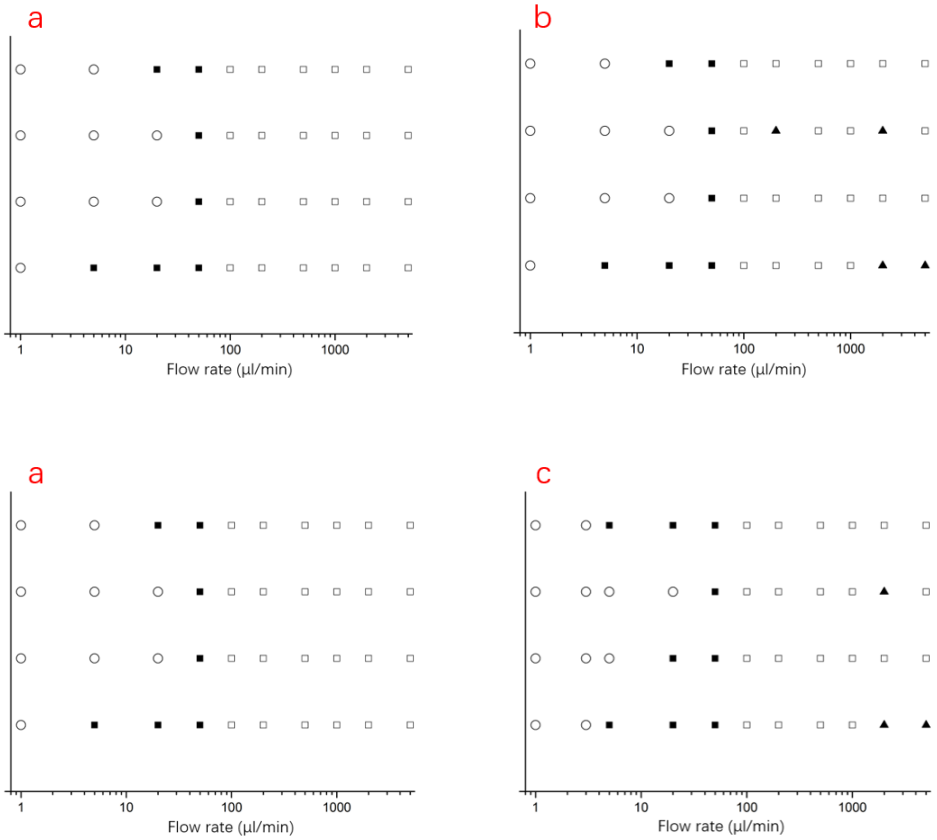

Figure 16. **(a)** is four times test for 400µm particles with 150 nm silica coating carried by the receding. **(b)** is 400 µm particles without coating. **(c)** is four tests of 150 µm 150 nm silica-coated particles contacted by receding interfaces. Circles indicate interface pinning, squares are for stick-slip motion, triangles for stick-slip motion vertical detachment. Solids symbols mean no horizontal detachment observed and open symbols indicate droplet leaves the interface during the movement.

4.1.2. Possible explanations for observations

To give an explanation for the observations, forces applying on the particle should be estimated. First to calculate the adhesion force (F_A), the Hamaker constant for SiO_2 and ETPTA (ester with acrylic acid) are taken as 10^{-20} J[37,38]. According to equation (4), the van der Waals attraction force for 400 µm particles is 0.83×10^{-5} N and 0.3125×10^{-5} N for 150 µm particles. For the aqueous phase which contains sodium thiosulfate, $1/k = 0.17\ nm$, while for aqueous phase with 16.7 wt.% sodium thiosulfate the

Debye length is 0.25 nm for aqueous phase with 6.8 wt.% sodium thiosulfate. Due to the high ionic strength, the calculated double layer force is small compared to the van der Waals attraction force (~10^{-9} N) when the deposited particle is immersed in oil and keeps increasing when the aqueous phase gradually submerges the particle (~10^{-6} N). In this case we take the van der Waals force as the maximum attraction force F_A to calculate the adhesion force on the particle.

To estimate the hydrodynamic driving force due to the flowrate, we consider a plug flow and constant shear rate, equation (19) and (20) is applied and take z as the particle diameter. With these approximations, we obtain that F_D ranges from 4.2x10^{-14} N to 2.8x10^{-6} N, but for low rate from 1μl/min to 1000μl/min, F_D is always negligible compared to the y-component of surface tension.

According to equation (21), gravity of the particle is in ~10^{7} N, which could be smaller when the particle is immersed in liquid phase because buoyancy will act on the particle and is negligible in our system.

The contact angle θ_p is measured from the contact angle of a droplet from the aqueous phase deposited on a plate that has a same composition with the particle under the oil phase and is shown in **Figure 17**. The contact angle of the plate, θ, is measured to be 40° for a receding interface and 97° for an advancing interface. We take friction factor as 0.1 for pure ETPTA particles and 0.3 for silica-coated particles and then we can get a graph of the maximum driving force and resistance

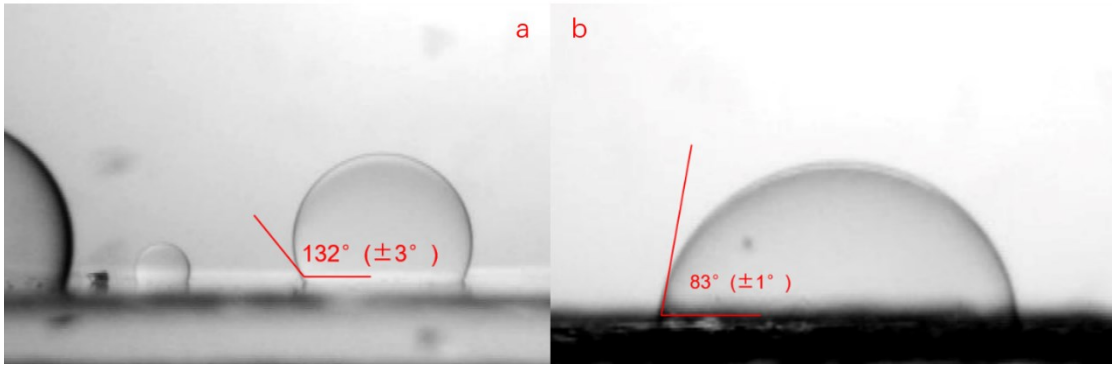

Figure 17. (**a)** Contact angle of aqueous phase in oil on pure ETPTA surface. **(b)** Contact angle measure on silica-coated ETPTA surface. Not much difference observed for different sized silica particles.

Then we can get a table for driving force and resistance.

Table 2. Forces applied on different particles

	400 μm ETPTA particle	150 μm ETPTA particle	400 μm silica-coated particle	150 μm silica-coated particle
F_γ^y at advancing interface (N)	$0.43*10^{-5}$	$0.16*10^{-5}$	$1.36*10^{-5}$	$0.51*10^{-5}$
Resistance at advancing interface (N)	$0.77*10^{-6}$	$0.29*10^{-6}$	$2.91*10^{-6}$	$1.1*10^{-6}$
F_γ^y at receding interface (N)	$1.54*10^{-5}$	$0.58*10^{-5}$	$1.0*10^{-5}$	$0.375*10^{-5}$
Resistance at receding interface (N)	$2.7*10^{-6}$	$1*10^{-6}$	$0.6*10^{-6}$	$22.8*10^{-6}$

It's obvious from the table that driving force is always larger than the resistance, so theoretically, the particle will always be affected by the liquid-liquid interface. Here are two assumptions. First, we assume that the contact angle of the interface at the particle and at the glass tubing is not constant for different flow rates. The dynamic contact angle will change the surface tension force as well as the capillary pressure force acting on the particle. So here we plot θ against θ_p and predict the particle behavior, then we get **Figure 18.**

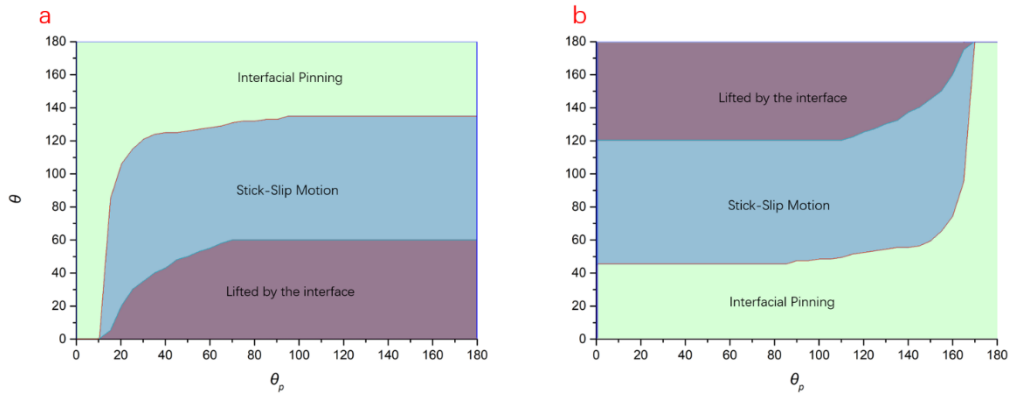

Figure 18. Prediction of particle mobilization for pure ETPTA particles based on the two surface tension force maxima. **(a)** for $\varphi > \theta_p$, **(b)** for $\varphi < \theta_p$. Pinning area and stick-slip motion boundary is defined by net force horizontally when total driving force $(F_\gamma^y + F_D) > 0$. The lifted area is defined by net vertical force $\left(F_\gamma^z + F_A\right) < 0$.

This gives a basic view of relationships between the two contact angles. From **Figure 18** we can tell the interfacial pinning region exists and is predictable for if we have the dynamic contact angle varying with the flow rate. The relationship between apparent contact angle (θ_{app}) and "microscopic" contact angle (θ_m) from microscopic properties of the contact line was studied and given by: [39]

$$\theta_{app}^3 = \theta_m^3 + Caln(0.16R/\theta_{app}L) \quad , \tag{31}$$

R is radius of curvature of the resulting meniscus, L is characteristic length set by microscopic effects like slip, a diffuse interface, or long-ranged forces. Ca is capillary number of the interface and is defined as:[40]

$$Ca = \mu u/\gamma \quad , \tag{32}$$

Where μ is fluid's dynamic viscosity, u is characteristic velocity.

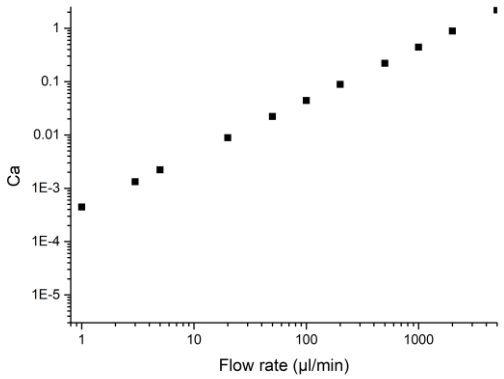

Figure 19. Capillary number of the oil-water interface.

The contact angle θ for receding interface and advancing interface in the experiment is given in **Figure 20**. As is shown in **Figure 18** and **Figure 20**, when flow rate increases, θ will increase for receding interface and decrease for an advancing interface, which will result in a vertical detachment .

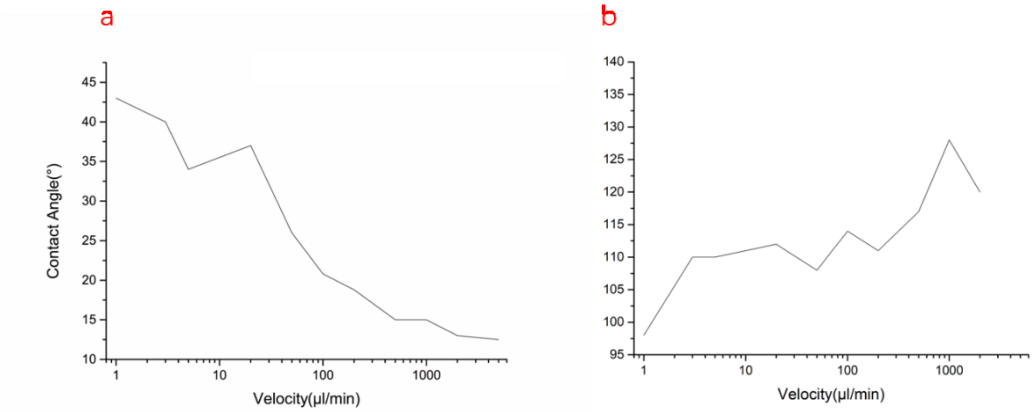

Figure 20. Contact angle measured from higher-wettability fluid side. **(a)** for a receding interface and **(b)** for an advancing interface.

The surface tension also depends on φ when the interface moves past the particle. For a fixed particle on the plate, since there is an equilibrium position for the interface on the particle surface and two maximum tension positions for $\varphi < \theta_p$ and $\varphi > \theta_p$, at the moment the interface touches the particle, the surface tension starts from zero to one maximum value then decrease to zero again when the interface reaches the equilibrium position. After that it will increase to another maximum value and decrease

to zero when the interface leaves the particle. If the particle is not fixed on the plate, at a moment the particle will start moving with the interface until the it moves back to the equilibrium position or the position where the tension cannot overcome the resistance. If we take the interface as the reference, the particle is oscillating at the interface. If we keep increasing the flow rate and at a moment the interface moves fast enough so that the surface tension will not be enough to overcome the resistance or as we can tell from the contact angle that two liquids have different wettability on the particle, there is a moment when the high-wettability phase takes over the dominant position, the particle will tend to decrease its surface energy and as a result, the particle will roll into the high-wettability phase and leave the interface. This can explain why pure ETPTA particle will have stick-slip motion with horizontal detachment when driven by the advancing interface that silicone oil has a higher wettability on the particle surface (silica-coated particles the opposite).

For higher flow rate when vertical detachment happens, the driving force exerted on the particle by the flow is not negligible. Also, formation of drops of low-wettability liquid immersed in high-wettability liquid is observed. Torques on the particle will have significant effect on particle motion and the local orientation of the liquid-liquid interface cannot be assumed solely by the contact angle at the wall. Surface properties will have greater influence on particle behaviors since there is a rotation, for the friction will switch from sliding friction to rolling friction and it will cause a disturbance around the particle. It will require further study to explain the phenomenon.

However, we still don’t have a precise model to predict the particle behaviors for

there are too many assumptions in this essay. First the DLVO theory for a particle that is partially immersed in oil and the rest in water is overly complicated (and likely unnecessary considering the high ionic strength). Dynamic contact angle is also hard to measuring *in situ* during the experiments but appears to be determining the dynamic regimes. Particles also have complex minute movements when in contact with the interface and affected by it. Minor local curvature will also have great influence on particle behaviors. A spontaneous absorption of the particle to the liquid-liquid interface is also observed as is shown in the figure which is also not interpreted in this work.

4.2. Interfacial tension tests and nucleation in oil

4.2.1. Test results and observations

Interfacial tension for ETPTA in air and water have been tested and great difference have been observed. By changing the filter, the influence of UV light and heat from the light bulb have been minimized. However, the surface tension remains increasing as is shown in **Figure 22**. To tell if it's related to droplets color change, ETPTA and water are uniformly mixed together and let the system rest for over 14 days so that the oil phase is transparent again. We take the water as ETPTA-saturated water and ETPTA as water-saturated ETPTA and monitor until the tension reaches an equilibrium. Surface tension for water-saturated ETPTA in fresh water and fresh ETPTA droplet in ETPTA-saturated water is shown in **Figure 23**. We can see from **Figure 23 (b)** that the surface tension remains stable for the latter case.

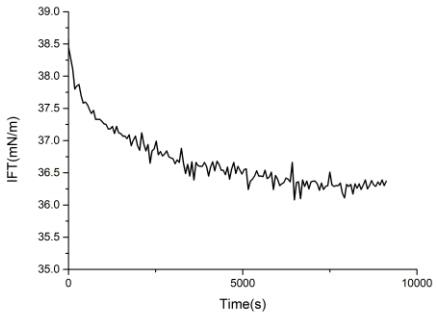

Figure 21. Interfacial tension of ETPTA in air.

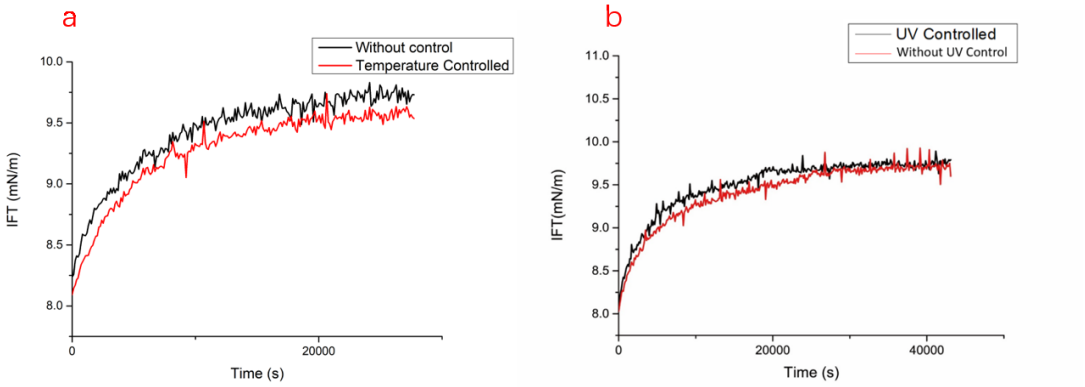

Figure 22. Interfacial tension of ETPTA droplets in water measured by device with modification. **(a)** is with heat shelter and **(b)** is the one with UV control.

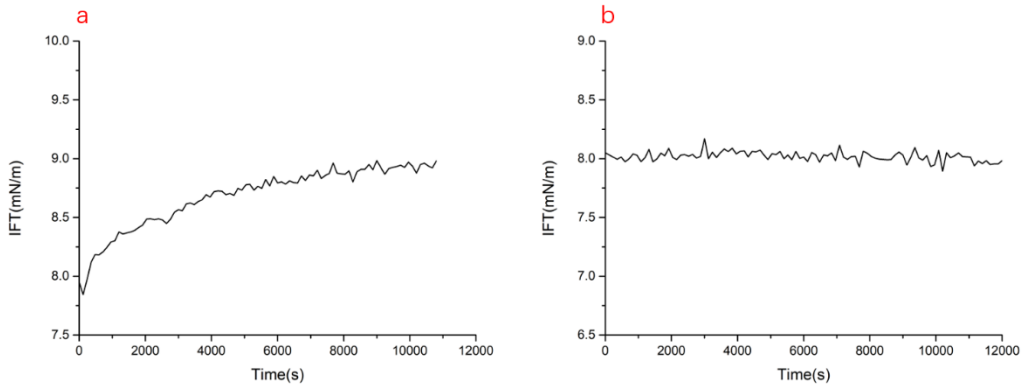

Figure 23. Interfacial tension measured for saturated systems. **(a)** is the tension of water-saturated ETPTA measured in fresh DI water. **(b)** is measured from a fresh ETPTA droplet from the bottle measured in ETPTA-saturated water, which is stable during the 12h-measurement.

For the O-ring device, the nucleation process is carefully recorded.

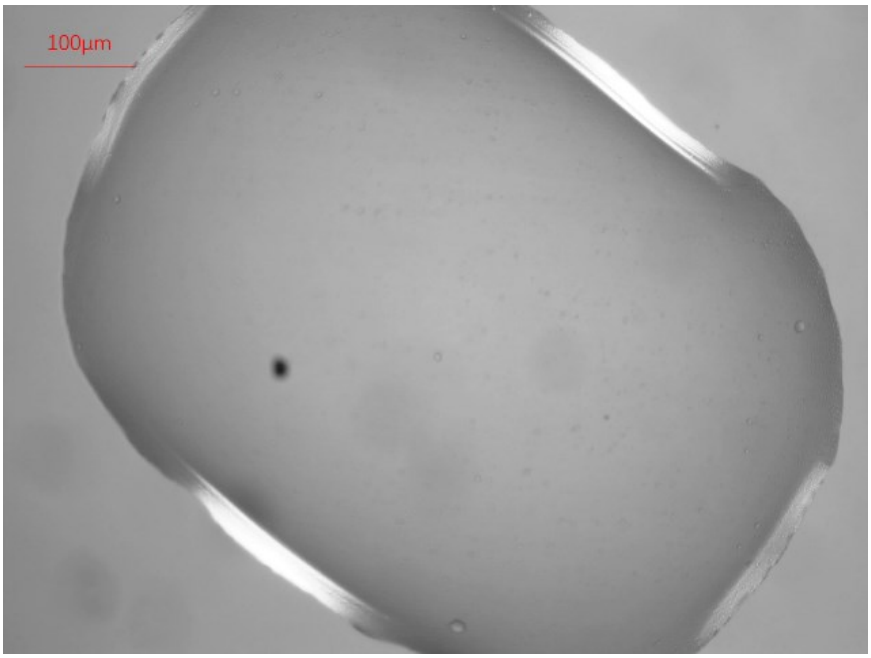

Figure 24. Microscopic photo of a ETPTA droplet in a O-ring-well device after 2 minutes.

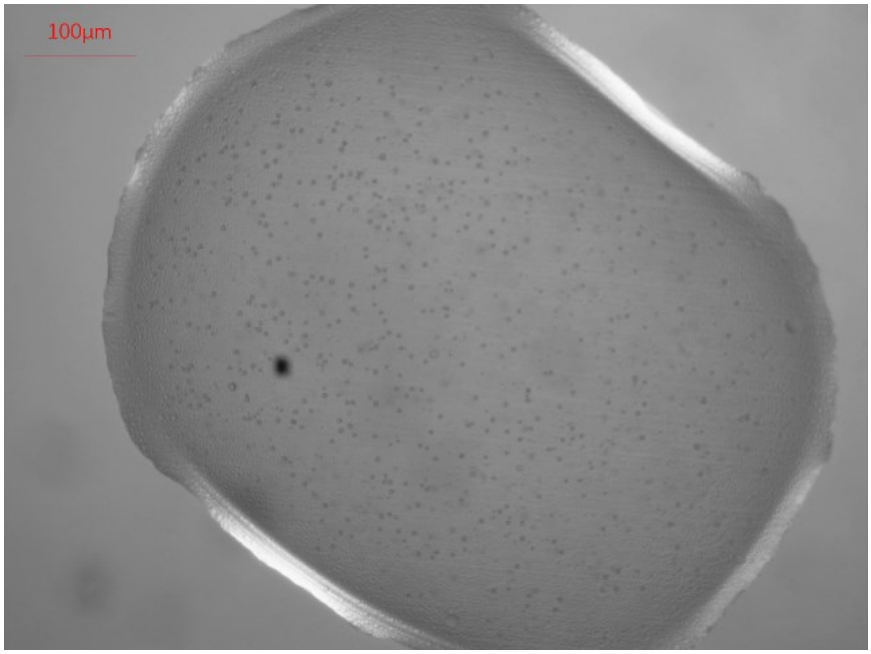

Figure 25. Microscopic photo of a ETPTA droplet in a O-ring-well device after 2 minutes.

The pictures and videos clearly show that water droplets nucleate from the edge to the center and from the solid-oil interface to the bulk oil phase. After switching the container from glass vial to a PMMA cuvette, the turbidity mainly occurs at the oil-water interface and is much less than in the glass vial. After seven days, the turbidity in

the cuvette is almost gone while not for the in the glass vial. For those containers with salt in the aqueous phase, ETPTA droplets remain transparent for a long time.

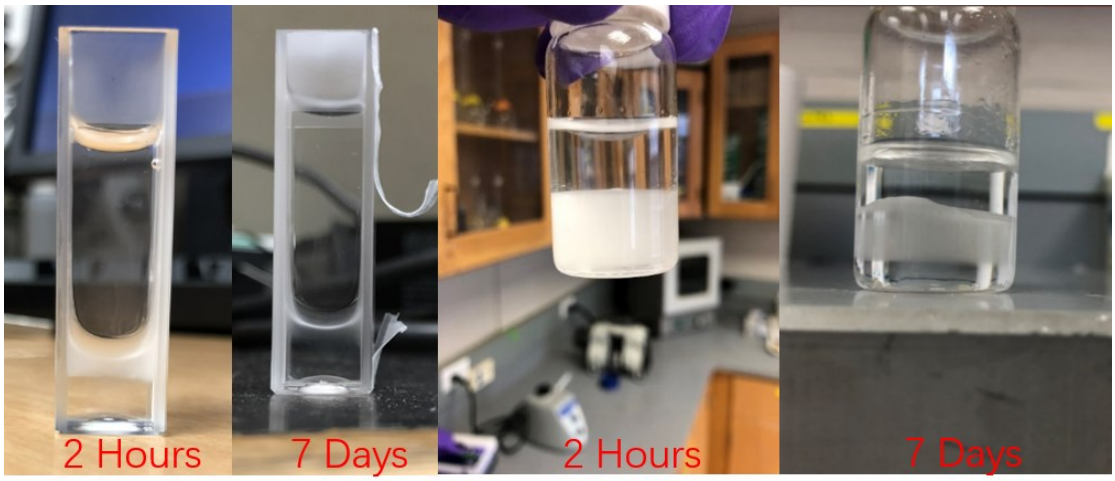

Figure 26. Containers for a mixture of ETPTA and water. For each container, ETPTA is the bottom phase and water is the upper phase. From left to right: mixture of ETPTA and water in PMMA cuvette after 2 hours' rest; mixture of ETPTA and water in PMMA cuvette after 7 days' rest; mixture of ETPTA and water in glass vial after 2 hours' rest; mixture of ETPTA and water in glass vial after 7 days' rest.

Figure 27. ETPTA droplets in glass vials with water and 400mM NaCl solution. Both liquids are of same amount for different devices.

4.2.2. Result discussion and possible assumptions

From the observation we can see that high salt concentration can keep the oil phase

transparent. However, if it's related to surface tension change is still not clear. To better understand the relations between color change and surface tension change, ETPTA's surface tension in 400mM NaCl water solution is tested. From the result we can tell the the tension is still increasing while the color for the oil droplet has no visible variation. Also if we take a ETPTA droplet from previous saturated system's bottom layer and lift it up to the upper aqueous phase then measure the interfacial tension, it will stay stable at the starting value along with a color change. During the process, the interface and the droplet get cloudy again and leaves a trail at the needle. This separate the surface tension change from the color change. The process is shown in **Figure 29**.

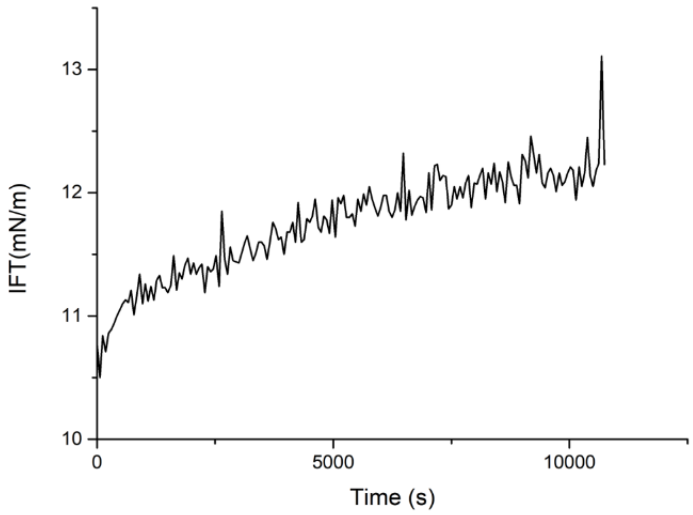

Figure 28. Interfacial tension for ETPTA droplet in 400mM NaCl solution

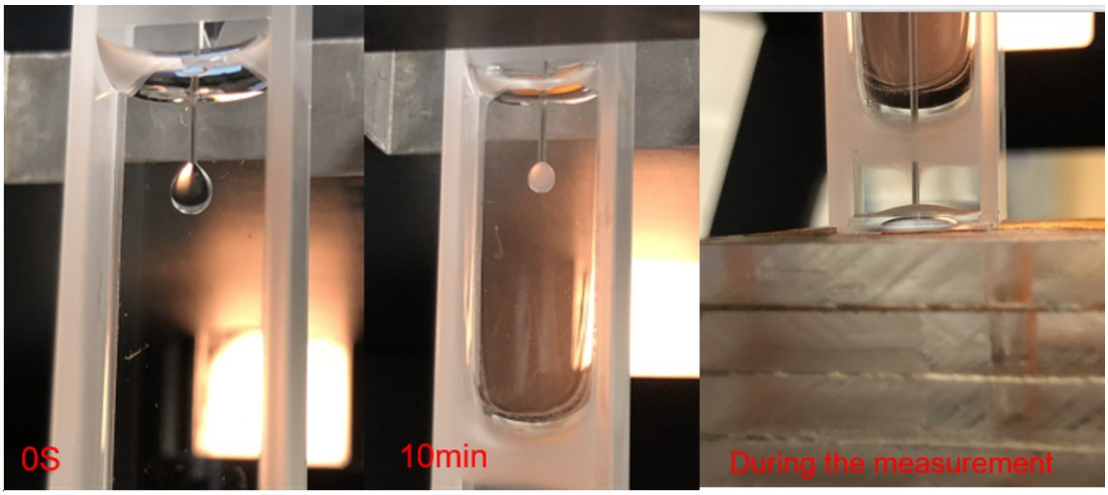

Figure 29. Surface tension measurement process for previous saturated system with ETPTA as bottom layer and water as upper layer. A drop of ETPTA is sucked up from the clear part at the bottom of the cuvette and measure the tension in upper water phase. The system had rest for 14days before the measurement.

Differences between the glass-vial-system and PMMA-cuvette-system shows nucleation mostly happens at solid-oil interface but also at oil-water interface. Color change of the oil comes from the nucleation of water in the oil phase, when both phases first meet together or a turbulence occurs at the interface, molecules diffuse into the other phase at a higher speed and exceed the solubility. Then the nucleation takes place at a relatively high speed. With water droplets keeps formation, a turbidity will be observed in oil phase. Presentation of salt will prevent this from happening.

5. CONCLUSIONS

This work mainly focused on the motion of a particle deposited on a solid surface as a liquid-liquid interface moves past it. Experimental observations have proved the existence of particle behaviors like interfacial pinning predicted by simulations in previous work. Also for both kinds of particles we have, interfacial pinning has been observed when the flow rate in the glass tubing is relatively low. As flow rate increases, particles will have stick-slip motion. For pure ETPTA droplets carried by the advancing interface and silica-coated droplets carried by the receding interface, a detachment alongside the plate is observed, particles will stay in the fluid with higher wettability. Vertical detachment (rolling induced jumping) is observed at high flow rate region and happens more frequently with smaller particles and ETPTA particles without silica coating.

Force balance calculation in the essay gives a brief explanation to why different types of particle motion is observed when varying the flow rate. Influence for different contact angles on the particle motion during the dynamic process is mentioned however precise model is not presented in this work. A more exact model for adhesion force of a partially immersed particle to a plate is required together with the dynamic contact angle.

Different sized silica coated particles don’t show much difference in behaviors. Surface roughness in this system is not a key variation in particle motion driven by the liquid-liquid interface. Hydrophilicity and hydrophobicity, however, plays a key role in predicting particle motion, which is valuable in industrial process.

The second part talks about the surface tension increase of ETPTA droplet in water. It is caused from ETPTA's dissolving in water as is explained in this essay. The surface tension is stable for both fresh ETPTA and water-saturated ETPTA in ETPTA-saturated water. Color changing results from water nucleation in oil. The nucleation mainly happens at solid-oil interface but also at oil-water interface, which can be controlled and prevented by adding salt to the aqueous phase. It's a cyclic process and will gradually tend to equilibrium. This could be useful in future research of ETPTA's properties in water and help built the model for particle motion

6. REFERENCE

1 McCarthy, J. F. & McKay, L. D. Colloid Transport in the Subsurface: Past, Present, and Future Challenges. *Vadose Zone Journal* **3**, 326-337, doi:10.2113/3.2.326 %J Vadose Zone Journal (2004).

2 Ochi, J. & Vernoux, J.-F. J. J. o. h. Permeability decrease in sandstone reservoirs by fluid injection: hydrodynamic and chemical effects. **208**, 237-248 (1998).

3 Cheng, T. & Saiers, J. E. J. W. R. R. Mobilization and transport of in situ colloids during drainage and imbibition of partially saturated sediments. **45** (2009).

4 Tufenkji, N. & Elimelech, M. J. L. Breakdown of colloid filtration theory: Role of the secondary energy minimum and surface charge heterogeneities. **21**, 841-852 (2005).

5 Yin, T., Shin, D., Frechette, J., Colosqui, C. E. & Drazer, G. J. P. r. l. Dynamic Effects on the Mobilization of a Deposited Nanoparticle by a Moving Liquid-Liquid Interface. **121**, 238002 (2018).

6 Bradford, S. A. & Torkzaban, S. J. V. Z. J. Colloid transport and retention in unsaturated porous media: A review of interface-, collector-, and pore-scale processes and models. **7**, 667-681 (2008).

7 Fogden, A., Kumar, M., Morrow, N. R., Buckley, J. S. J. E. & Fuels. Mobilization of fine particles during flooding of sandstones and possible relations to enhanced oil recovery. **25**, 1605-1616 (2011).

8 Lenhart, J. J., Saiers, J. E. J. E. s. & technology. Transport of silica colloids through unsaturated porous media: Experimental results and model

comparisons. **36**, 769-777 (2002).

9 Aramrak, S., Flury, M., Harsh, J. B., Zollars, R. L. J. E. s. & technology. Colloid mobilization and transport during capillary fringe fluctuations. **48**, 7272-7279 (2014).

10 Zhang, Q. & Hassanizadeh, S. M. J. C. E. S. The role of interfacial tension in colloid retention and remobilization during two-phase flow in a polydimethylsiloxane micro-model. **168**, 437-443 (2017).

11 Stöber, W., Fink, A., Bohn, E. J. J. o. c. & science, i. Controlled growth of monodisperse silica spheres in the micron size range. **26**, 62-69 (1968).

12 Plimpton, S. J. J. o. c. p. Fast parallel algorithms for short-range molecular dynamics. **117**, 1-19 (1995).

13 Lazouskaya, V. *et al.* Colloid mobilization by fluid displacement fronts in channels. **406**, 44-50 (2013).

14 Gómez-Suárez, C., van der Mei, H. C., Busscher, H. J. J. C., Physicochemical, S. A. & Aspects, E. Air bubble-induced detachment of polystyrene particles with different sizes from collector surfaces in a parallel plate flow chamber. **186**, 211-219 (2001).

15 Gómez-Suárez, C., Busscher, H. J. & van der Mei, H. C. J. A. E. M. Analysis of bacterial detachment from substratum surfaces by the passage of air-liquid interfaces. **67**, 2531-2537 (2001).

16 Boks, N. P. *et al.* Mobile and immobile adhesion of staphylococcal strains to hydrophilic and hydrophobic surfaces. **331**, 60-64 (2009).

17 Sogah, D. Y., Hertler, W. R., Webster, O. W. & Cohen, G. M. J. M. Group transfer polymerization-polymerization of acrylic monomers. **20**, 1473-1488 (1987).

18 Derjaguin, B. & Landau, L. Theory of the stability of strongly charged lyophobic sols and the adhesion of strongly charged particles in solutions of electrolytes: Acta Physicochim URSS, v. 14. (1941).

19 Yoon, R.-H., Mao, L. J. J. o. C. & Science, I. Application of extended DLVO theory, IV: derivation of flotation rate equation from first principles. **181**, 613-626 (1996).

20 Verwey, E. & Overbeek, J. T. G. (Amsterdam Holland, 1948).

21 Israelachvili, J. N. *Intermolecular and surface forces*. (Academic press, 2011).

22 Derjaguin, B. v. & Landau, L. J. P. i. S. S. Theory of the stability of strongly charged lyophobic sols and of the adhesion of strongly charged particles in solutions of electrolytes. **43**, 30-59 (1993).

23 London, F. J. T. o. t. F. S. The general theory of molecular forces. **33**, 8b-26 (1937).

24 Derjaguin, B. J. C. & science, p. Untersuchungen über die Reibung und Adhäsion, IV. **69**, 155-164 (1934).

25 Leenaars, A. in *Particles on Surfaces 1* 361-372 (Springer, 1988).

26 Goldman, A. J., Cox, R. G. & Brenner, H. J. C. e. s. Slow viscous motion of a sphere parallel to a plane wall—I Motion through a quiescent fluid. **22**, 637-651 (1967).

27 O'neill, M. J. C. E. S. A sphere in contact with a plane wall in a slow linear shear flow. **23**, 1293-1298 (1968).

28 Kobayashi, Y. *et al.* Silica coating of silver nanoparticles using a modified Stöber method. **283**, 392-396 (2005).

29 Zhang, S., Li, G.-L., Cong, H.-L., Yu, B. & Gai, X.-Y. J. I. F. Size control of monodisperse silica particles by modified Stöber method. **178**, 52-57 (2017).

30 Boissière, C., Van Der Lee, A., El Mansouri, A., Larbot, A. & Prouzet, E. J. C. C. A double step synthesis of mesoporous micrometric spherical MSU-X silica particles. 2047-2048 (1999).

31 Lei, X. *et al.* Synthesis of monodisperse silica microspheres by a modified stöber method. **154**, 142-146 (2014).

32 Van Blaaderen, A., Van Geest, J., Vrij, A. J. J. o. c. & science, i. Monodisperse colloidal silica spheres from tetraalkoxysilanes: particle formation and growth mechanism. **154**, 481-501 (1992).

33 Pickering, S. U. J. J. o. t. C. S., Transactions. Cxcvi.—emulsions. **91**, 2001-2021 (1907).

34 Yang, Z. & Abbott, N. L. J. L. Spontaneous formation of water droplets at oil−solid interfaces. **26**, 13797-13804 (2010).

35 Zhang, X. H. & Ducker, W. J. L. Interfacial oil droplets. **24**, 110-115 (2008).

36 Anand, S., Rykaczewski, K., Subramanyam, S. B., Beysens, D. & Varanasi, K. K. J. S. m. How droplets nucleate and grow on liquids and liquid impregnated surfaces. **11**, 69-80 (2015).

37 Tsai, C.-J., Pui, D. Y., Liu, B. Y. J. A. S. & Technology. Elastic flattening and particle adhesion. **15**, 239-255 (1991).

38 Bergström, L. J. A. i. c. & science, i. Hamaker constants of inorganic materials. **70**, 125-169 (1997).

39 Bonn, D., Eggers, J., Indekeu, J., Meunier, J. & Rolley, E. J. R. o. m. p. Wetting and spreading. **81**, 739 (2009).

40 Shi, Z. *et al.* Dynamic contact angle hysteresis in liquid bridges. **555**, 365-371 (2018).

7. CURRICULUM VITAE

Name: Tianxu Huang

Birth: Feb, 15, 1995, Daqing, China

Address: Tianxu Huang may be contacted through Dr. Joelle Frechette at the Chemical and Biomolecular Engineering Department, Johns Hopkins University, Baltimore, MD 21218

Email Address: huangtianxu0215@gmail.com

Education: B.Eng., Chemical Industry and Engineering Technology, Tianjin University, 2017

Research:

High-energy Fuel Research Group

April 2014~July 2017

Research on Preparing Fe-TiO2 Quantum Dots by Loading Method and Its Photocatalytic Reaction

April 2015~July 2016

Preparation of Ni-P Catalyst and Its Application in HER and OER

November 2016~July 2017

Multi-Component Assembly Based on Peptide Molecular

April 2015~June 2017